Article

Not peer-reviewed version

Targeting the Melanocortin 1 Receptor in Melanoma: Biological Activity of α-MSH Peptide Conjugates

Ildikó Szabó , Beata Biri-Kovács , Balázs Vári , Ivan Ranđelović , Diána Vári-Mező , Éva Juhász , Gábor Halmos , Szilvia Bősze , József Tóvári , Gábor Mező *

Posted Date: 27 November 2023

doi: 10.20944/preprints202311.1667.v1

Keywords: α-MSH; melanoma; peptide-drug conjugates; in vitro antiproliferative effect; in vivo antitumor activity

Article

Targeting the Melanocortin 1 Receptor in Melanoma: Biological Activity of α-MSH Peptide Conjugates

Ildikó Szabó [1,2], Beáta Biri-Kovács [1], Balázs Vári [3,4,#], Ivan Ranđelović [3,#], Diána Vári-Mező [1,3,4], Éva Juhász [5], Gábor Halmos [6], Szilvia Bősze [1], József Tóvári [3,4,#] and Gábor Mező [1,7,*,#]

[1] HUN-REN–ELTE Research Group of Peptide Chemistry, Budapest, Hungary
[2] MTA-TTK "Momentum" Peptide-Based Vaccines Research Group, Institute of Materials and Environmental Chemistry, HUN-REN Research Centre for Natural Sciences, Budapest, Hungary; biri.beata@gmail.com
[3] Department of Experimental Pharmacology and National Tumor Biology Laboratory, National Institute of Oncology, Budapest, Hungary
[4] School of Ph.D. Studies, Semmelweis University, Budapest, Hungary
[5] Department of Pediatrics, Faculty of Medicine, University of Debrecen, Debrecen, Hungary
[6] Department of Biopharmacy, Faculty of Pharmacy, University of Debrecen, Debrecen, Hungary
[7] Institute of Chemistry, Eötvös Loránd University, Budapest, Hungary
* Correspondence: gabor.mezo@ttk.elte.hu
# Consortium members of European Union's Horizon 2020 research and innovation program under the Marie Skłodowska-Curie grant agreement No 861316

Abstract: Malignant melanoma is one of the most aggressive and resistant tumor types which is often accompanied by poor prognosis when spread to nearby or distant tissues. Even though an increasing number of second-line therapies are available for cancer patients, the 5-year survival rate of melanoma patients with regional and distant metastases is still rather low. Therefore, there is an urgent need to develop new, highly efficient treatments. Melanocortin-1-receptor (MC1R) is a cell surface receptor for α-MSH. It is responsible for melanogenesis and is shown to be overexpressed on the surface of cancer cells in a subset of melanoma patients. Here, we designed and synthesized α-MSH analogs and conjugated them to daunomycin through oxime linkage. Using our peptide-drug conjugates (Dau-α-MSHs), we performed comparative in vitro and in vivo evaluations to reveal their suitability for tumor targeting. Firstly, the expression level of MC1R was determined in various melanoma cell lines via RT-qPCR. Then, we examined the antiproliferative effect of our Dau-α-MSHs, moreover we determined the cellular uptake profile and intracellular localization of Dau-α-MSHs. The most efficient Dau-α-MSHs were investigated in vivo using a murine xenograft melanoma model. We found that various cell lines show differential expression on the mRNA levels. We also showed that healthy primary cells have lower expression of MC1R compared to tumor cell lines. Moreover, the concentration-dependent cellular uptake profile of Dau-α-MSHs was detected and the compounds exhibited a great antiproliferative effect on melanoma cell lines. We also provided evidence that our novel Dau-α-MSHs can inhibit tumor expansion significantly and are suitable for targeted tumor therapy.

Keywords: α-MSH; melanoma; peptide-drug conjugates; in vitro antiproliferative effect; in vivo antitumor activity

1. Introduction

Melanoma is one of the three main types of skin cancer. Although melanoma is much less common than other skin cancers (it accounts for ~21% of all skin cancer incidences) [1], its extremely aggressive behavior makes it the leading cause of death among tumors of the skin. Melanoma originates from the malignant transformation of melanocytes, which are the melanin- producing cells of the skin, hair, and eyes. It is formed either by dysfunction of dysplastic nevi or a single melanocyte

 doi:10.20944/preprints202311.1667.v1

[2]. Melanocytes locates with the keratinocytes in the basal layer of the epidermis and form a very stable population, as they proliferate extremely rarely under normal circumstances. Not only the outer layer (epidermis), but the inner layer (dermis) of the skin (that involves hair roots, blood, lymph vessels, and nerves) as well includes melanocytes, but they are a biologically different population compared to the ones located in the epidermis. Since its first recognition by Clark *et al.* [3], melanoma is heterogeneous, comprising a population of melanocytes of different origins and differentiation stages (from undifferentiated cancer stem cells with self-renewal-, high proliferation and differentiation capacity to functional melanocytes). Therefore, each melanoma variant behaves differently and has a different prognosis, which implies that there is no uniform treatment that can be used effectively [3]. Furthermore, because of their location, melanocytes have a high potential to spread rapidly to other parts of the body by entering the lymphatic system and bloodstream resulting in a high rate of developing metastasis.

Although chemotherapy is the main treatment procedure for cancers, it is mostly ineffective for advanced melanoma due to its several intrinsic and/or extrinsic resistances to traditional antineoplastic agents [4]. Since the middle of the 20th century, there has been intensive research for the development and testing of potential chemotherapeutic agents that were reviewed by Yang et al. [5], e.g. dacarbazine, its analog temozolomide, and melphalan. Dacarbazine was uniquely, without clinical trials, approved by the FDA in 1975 for the treatment of melanoma. It is the only FDA-approved chemotherapeutic drug for melanoma, but its efficacy is far from what is desired. Dacarbazine used alone as a single therapeutic agent does not result in significant survival. Less than 2% of treated patients survived up to 6 years [6]. Temozolomide, an orally administered dacarbazine derivative, has very similar efficacy as dacarbazine [7]. Temozolomide can penetrate to the central nervous system (CNS) therefore, it has been suggested for the prevention and treatment of brain metastases. However, it was quickly demonstrated in phase III clinical trials that its application did not show any benefit in the treatment of brain metastases [8]. At that time, another alkylating agent, the nitrogen mustard derivative melphalan, was also an intensively researched antineoplastic agent. In 1968, the first clinical trials of chemotherapy for metastatic melanoma were conducted with melphalan, but it failed because of its narrow therapeutic window [9–11].

The melanocortin 1 receptor (MC1R), a G-protein coupled receptor, has a pivotal role in melanogenesis and skin pigmentation due to the binding of its ligand, α-Melanocyte Stimulating Hormone (α-MSH). Physiologically, more than 80 variants of MC1R have been recently described in the Caucasian population [12]. Some of these variants result in a partial loss of receptor signaling ability, as they are not able to stimulate cyclic adenosine monophosphate (cAMP) production as strongly as the wild-type receptor when stimulated by α-MSH [13,14]. This molecular alteration underlies the "red hair color" (RHC) phenotype, which is characterized by light pigmentation and sun sensitivity. Furthermore, this phenotype has a higher risk for melanoma compared to the wild-type MC1R-carrying individuals [15–24]. While the MC1R expression level is much lower in healthy melanocytes, melanoma cells frequently overexpress it. Therefore, this makes MC1R a useful marker for malignant melanoma as well as a potential target for melanoma diagnosis and therapy [25–29].

Peptide hormones, such as α-MSH regulate skin pigmentation in most vertebrates. The core α-MSH sequence His^{6}-Phe^{7}-Arg^{8}-Trp^{9}, conserved in several species, is sufficient for receptor recognition [30], while the C-terminal fragment is not essential for receptor binding. The presence of α-MSH receptors (MC1R) on both murine and human melanoma cells [31] suggests that α-MSH analogs can be developed into targeted melanoma imaging or therapeutic agents [32,33]. In addition, the hormone-receptor complex is rapidly internalized, and the receptor undergoes recycling within a few minutes. Based on these facts, several α-MSH analogs, linear and cyclic as well, have been intensively developed and published. Among them, substitution of Met^{4} with Nle^{4} and Phe^{7} with D-Phe^{7} yielded one of the most effective α-MSH analogs with sub-nanomolar receptor binding affinity and resistance to enzymatic degradation [34–36]. The α-MSH analogs have been predominantly used as diagnostic tools in the field of melanoma research, but only a few research data present their chemotherapeutic applications [32,33,35,37–45]. However, the structure-activity relationship data obtained by diagnostic research provide an excellent basis for the preparation of conjugates for targeted drug

 doi:10.20944/preprints202311.1667.v1

delivery. The first melanoma targeting attempt was the synthesis and investigation of a β-MSH daunomycin conjugate. This conjugate was able to get into mouse melanoma cells by receptor-mediated endocytosis [46]. Süli-Vargha and colleagues focused on reducing the toxicity and avoiding drug resistance. They used not only the α-MSH analogs, but a series of their fragments, which have been coupled to or involved nitrosourea or melphalan to serve as drug conjugates for melanoma targeting [39,47]. These truncated α-MSH conjugates preserved receptor recognition, and some of them showed irreversible binding to the receptor as well, with selective and specific cytotoxic effect mediated by MC1R [35,46]. The improved efficacy and irreversible receptor binding of melphalan containing α-MSH conjugates can be explained by its alkylating feature. The extracellular N-terminal tail of the MC1R is responsible for ligand affinity [48] and signal anchoring [49,50]. At the junction of the N-terminal and the first transmembrane domain of the receptor, there is a cysteine residue, which is essentially required for receptor function [51,52]. It was also assumed that this cysteine residue might also serve as a target for melphalan or other kind of alkylating agents, which can react not only with the DNA but also with the thiol group of cysteine due to their alkylating ability, forming a very stable receptor-ligand complex (unpublished data).

In this manuscript, we report the synthesis, *in vitro*, and *in vivo* antitumor activity of novel α-MSH-based drug conjugates. Daunomycin as a chemotherapeutic agent was coupled to different α-MSH peptides (native and fragment) by oxime ligation. *In vitro* cytostatic activity, cellular uptake profile and intracellular localization of the peptide-drug conjugates were determined in different human melanoma cell cultures. Furthermore, we determined the effects of α-MSH drug conjugates on tumor growth and metastasis compared to the free daunomycin *in vivo*. These biological evaluations established the effective suitability of α-MSH derivatives as targeting units.

2. Results

Different α-MSH peptide derivatives were synthesized to produce peptide-drug conjugates. The native sequence (Ac-SYSMEHFRWGKPV-NH2) was used as a control with a slight modification. To avoid the unwanted oxidation of methionine during the synthesis, it was replaced with norleucine in the original sequence (Ac-SYSNleEHFRWGKPV-NH_2) which is allowed by the literature data [53–56]. The native sequence was also truncated by focusing on the central part of the peptide (NleEHfRWGK). In this truncated peptide, another modification was done to improve the receptor binding affinity. The central region of the peptide contains phenylalanine, which, according to the literature, can be replaced by its D-configuration counterpart [34–36].

2.1. Synthetic Procedures and Chemical Characterization

The synthesis of the α-MSH peptides- full-length as well as truncated ones- was carried out manually by solid-phase peptide synthesis using Fmoc/^{t}Bu strategy. To ensure drug conjugation, the peptides have been endowed with an aminooxy functional group by incorporation of the aminooxyacetyl group at different sites on the peptides. Peptides were cleaved from the resin with TFA in the presence of appropriate scavengers. Prior to the conjugation, the cleaved peptides without any purification were characterized by analytical RP-HPLC and ESI-HRMS. Oxime ligation between Aoa-α-MSH peptides and Dau was carried out in 0.2 M NaOAc solution (pH 5.2) at RT for 24 h. The following oxime-linked Dau-α-MSH conjugates were prepared: the drug was attached to the N-terminus of peptide (**Conj1**), or to the side chain of lysine in the sequence. In the latter case, the N-terminal part was acetylated (**Conj2** and **Conj4**, native and truncated ones, respectively). In addition, a conjugate containing two copies of the drug molecule was also developed (**Conj3**) (Figure 1.).

Preprints (www.preprints.org) | NOT PEER-REVIEWED | Posted: 27 November 2023 doi:10.20944/preprints202311.1667.v1

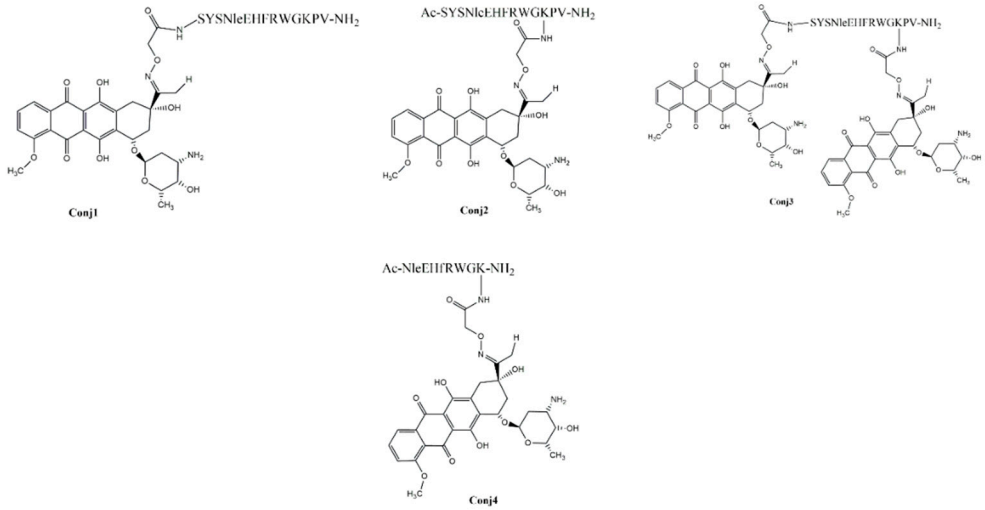

Figure 1. Chemical structure of the Dau-α-MSH conjugates.

The drug-containing conjugates were purified by semi-preparative RP-HPLC and characterized by analytical RP-HPLC and ESI-HRMS (Table 1 and SI Figure S1-S4).

Table 1. Chemical characterization of Dau-α-MSH peptide conjugates.

Code	Sequence	tR (min)[1]	Mmo (Da)[2]		differences (ppm)
			calc	meas	
Conj1	Dau=Aoa-SYSNleEHFRWGKPV-NH_2	12.6	2187.0266	2187.0080	18.56
Conj2	Ac-SYSNleEHFRWGK(Dau=Aoa)PV-NH_2	13.0	2229.0371	2229.0214	15.66
Conj3	Dau=Aoa-SYSNleEHFRWGK(Dau=Aoa)PV-NH_2	12.8	2769.2272	2769.6050	32.76
Conj4	Ac-NleEHfRWGK(Dau=Aoa)-NH_2	12.9	1694.7876	1694.7692	18.36

[1] Retention time on Phenomenex Jupiter C12 column, gradient: 5–100% B, 20 min. According to the high-performance liquid chromatography (HPLC) analysis, the purity of the conjugates was always above 95%. [2]Mmo meas. (monoisotopic molecular mass) measured on a Thermo Scientific Q Exactive Focus Hybrid Quadrupole-Orbitrap mass spectrometer.

2.2. Biological Characterization of the Full Length α-MSH Drug Conjugates

Firstly, we decided to determine and compare the *in vitro* and *in vivo* biological activity of Dau conjugates with the full-length α-MSH. For this purpose, the *in vitro* cytostatic activity and cellular uptake profile of the conjugates (**Conj1**, **2**, and **3**) were investigated. Furthermore their *in vivo* tumor growth inhibitory effect was also determined on mouse melanoma allograft and xenograft models.

2.2.1. In Vitro Antiproliferative Activity of Full Length α-MSH Drug Conjugates

In vitro studies of antiproliferative effect showed that melanoma targeting Dau-conjugates have significantly higher efficacy on B16 murine melanoma cell lines in comparison to human melanoma cell lines (A2058, M24, and WM983B). The IC_{50} values were detected between 2 and 2.9 μM on B16 cells, where the highest activity was detected in the case of conjugate **Conj3**, followed by **Conj2** and **Conj1** (Table 2). Moreover, the relative potency of conjugates to free Dau was also calculated as independent values from cell lines. A higher value of relative potency indicates elevated targeting capacity of the conjugate on particular cell lines. Considering relative potencies, the best targeting capacity showed to be **Conj3** on all four cell lines, followed by **Conj2** and **Conj1** (Table 2). The highest

 doi:10.20944/preprints202311.1667.v1

antitumor activity of **Conj3** on cells can be explained by the presence of two Dau molecules in this conjugate in comparison with **Conj2** and **Conj1** which contain only one drug molecule.

Table 2. *In vitro* antiproliferative activity of full length α-MSH drug conjugates.

Cell line	IC_{50}[1]				Relative potency[2]		
	Conj1 (μM)	**Conj2** (μM)	**Conj3** (μM)	**Dau** (nM)	**Conj1**	**Conj2**	**Conj3**
B16	2.9 ± 0.6	2.8 ± 0.7	2.0 ± 0.7	26.0 ± 8.0	0.0090	0.0093	0.0130
A2058	9.8 ± 5.4	3.2 ± 0.4	3.0 ± 0.8	40.0 ± 6.5	0.0041	0.0125	0.0133
M24	12.8 ± 1.6	11.5 ± 0.4	11.0 ± 0.8	118.8 ± 25.0	0.0093	0.0103	0.0108
WM983B	9.9 ± 1.5	7.9 ± 0.7	3.6 ± 0.2	49.8 ± 22.9	0.0050	0.0063	0.0138

[1] IC_{50} values (average ± SD) were determined by computerized curve-fitting program (Origin®2018). The cells were treated with the conjugates at 0.8-100μM concentration range for 24 h. After incubation, the cells were washed and cultured for 48 h in appropriate serum-containing cell culture medium for 48 h. On the fourth day, the MTT assay was carried out to determine the IC_{50} values of the compounds. Values shown are mean ± SD of two or three independent experiments, each performed in four parallels. [2] Relative potency was calculated as a ratio of IC_{50} values of free Dau and conjugates.

2.2.2. In Vitro Flow Cytometry Evaluation of Full Length α-MSH Drug Conjugates

To better understand the subcellular mechanism of the newly synthesized Dau-α-MSH conjugates, we decided to monitor their cellular uptake. This could be easily carried out because of the fluorescence propensity of Dau: its emission can be detected both by flow cytometry and fluorescence microscopy. For quantification of the cellular uptake, flow cytometry studies were performed. First, all conjugates (**Conj1**, **2**, and **3**) were monitored on A2058 cells in different concentrations (Figure 2). All conjugates were taken up in a concentration-dependent manner. **Conj2** and **Conj3** showed the highest intensity, but interestingly, no significantly higher fluorescence values were detected in the case of **Conj3** which contains two daunomycin molecules. Therefore, we can assume that **Conj2** can enter the cells most efficiently.

Considering the *in vitro* data, a good correlation was observed between the internalization ability and the cytostatic efficacy of the conjugates. **Conj1** with the lowest internalization ability has the highest IC_{50} value (9.8 ± 5.4μM), while **Conj2** and **Conj3**, which have similar cellular uptake ability, also have similar IC_{50} values (3.2 ± 0.4 and 3.0 ± 0.8 μM, respectively). Based on the *in vitro* data, it can be concluded that the attachment of the drug to the N-terminus of the α-MSH peptide (**Conj1**) is not preferred and neither of the two drug molecules (**Conj3**) enhances the *in vitro* efficacy of the conjugate.

Preprints (www.preprints.org) | NOT PEER-REVIEWED | Posted: 27 November 2023 doi:10.20944/preprints202311.1667.v1

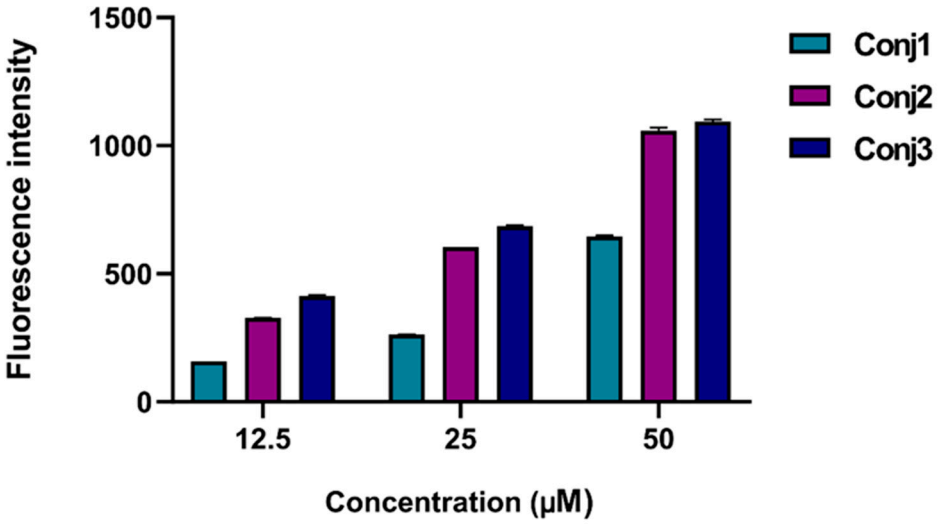

Figure 2. Determination of cellular uptake of Dau-α-MSH conjugates measured by flow cytometry. A2058 cells were treated with the conjugates in a 12.5-50 μM concentration range for 3 h. The increase of the fluorescence intensity of melanoma cells was monitored by flow cytometry (BD LSR II, BD Bioscience, San Jose, CA). Data was analyzed with FACSDiVa 5.0 software.

2.2.3. In Vivo Antitumor Effect of Full Length α-MSH Drug Conjugates on B16 Melanoma Model

Prior to the *in vivo* studies of the antitumor effect of conjugates, an *in vivo* acute toxicity study was performed on healthy mice with the representative conjugate **Conj2** to determine the treatment dose. After 14 days, no significant change in body weight (Figure S5), as well as in the general appearance and behavior of mice were observed. Based on the results, it was concluded that conjugate **Conj2** does not show acute toxicity for the animals up to the dose of 25 mg Dau content/kg, and that antitumor activity of Dau-α-MSH conjugates can be further investigated on tumor-bearing mice.

The effect of Dau-α-MSHs compared to the free drug was determined on subcutaneous B16 murine melanoma-bearing mice as a preliminary *in vivo* model. Animal body weight in control and treatment groups increased at the end of the experiment in comparison to the start. Increasing body weight of 9.4 and 7.6% was observed in control and free Dau groups, respectively, while **Conj1**, **Conj2**, and **Conj3** treated groups showed an increase of 12.9, 8.5 and 18.2 %, respectively (Figure 3a, and Table S1). During the experiment, one animal died in the control group, 3 animals in the group treated with free Dau, and 2 animals died in each group treated with Dau-α-MSH conjugates. The antitumor effect of melanoma targeting Dau-α-MSHs was evaluated by measuring both tumor volume and tumor weight in each group. Based on the tumor volume data presented in mm^3, it was observed at the end of the experiment that the most potent conjugate (**Conj2**) inhibited the tumor growth by 37.8%, while **Conj1** inhibited it by 23.8% (Figure 3b, Table S1). A slight numeric (4.9%) inhibition was detected in the case of free Dau treatment, while surprisingly the average tumor volume size in the **Conj3** treated group was 12.3% higher compared to the control group. Setting arbitrarily all tumor volumes as 100% at the starting point of the treatment, and following their percentage growth, the highest tumor growth inhibition was also determined in the case of the **Conj2** treated group (75.4 % that was more pronounced by this type of calculation), then in **Conj3** treated group (14.7 % inhibition), while the tumor volume in **Conj1** and free Dau treated groups increased by 9.7 and 58.8%, respectively, in comparison to the control group (Figure 3c, Table S1). Additionally, the antitumor effect of melanoma targeting Dau-α-MSH conjugates was evaluated by measuring tumor weight in each group after termination of the experiment (Figure 3d, Table S1). Based on tumor weight we could obtain that **Conj2** showed the highest inhibition again, which inhibited tumor growth by 38.6% in comparison to the control group. Free Dau inhibited tumor growth by 17% and

Preprints (www.preprints.org) | NOT PEER-REVIEWED | Posted: 27 November 2023 doi:10.20944/preprints202311.1667.v1

Conj1 by 2.4%, while tumor weight in the **Conj3** treated group was increased by 9.2% in comparison to the control.

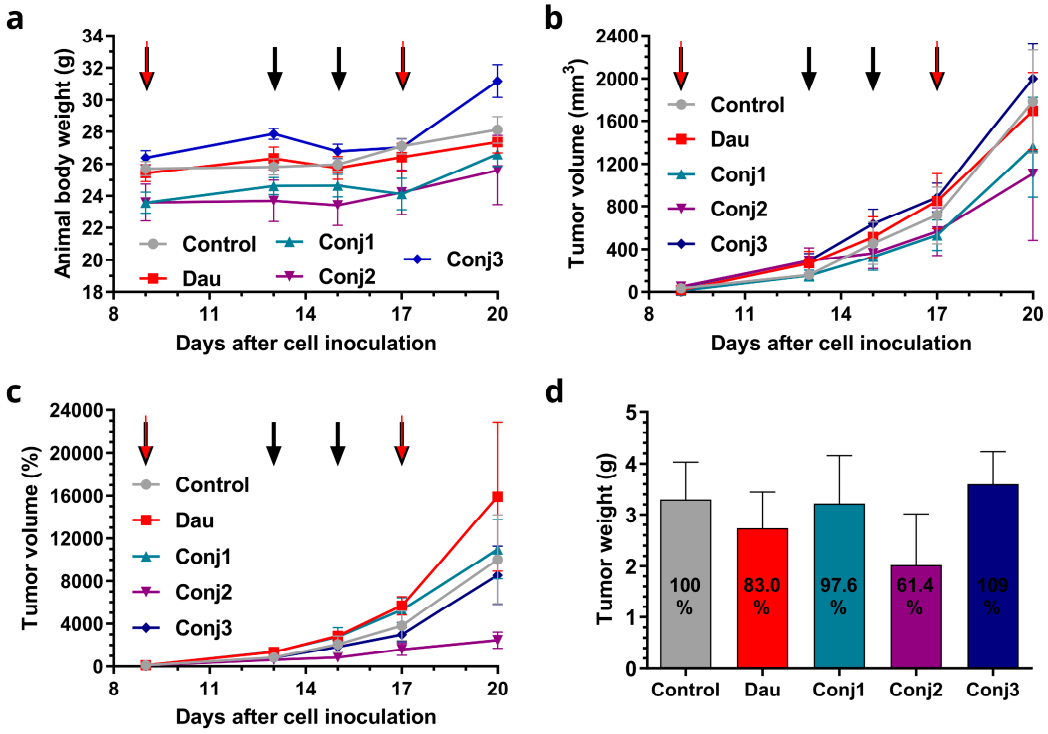

Figure 3. Effect of Dau-α-MSH conjugates (10 mg Dau content/kg, black arrows) and free Dau (1 mg /kg, red arrows) in subcutaneous B16 murine melanoma bearing C57BL/6 male mice in vivo. (**a**) Animal body weight (grams, average ± SEM). (**b**) Tumor volume (mm3, average ± SEM). (**c**) Tumor volume (percentage, average ± SEM). (**d**) Tumor weight (grams, average ± SEM). 7 animals per group.

To conclude the results, **Conj2** exhibits the highest antitumor effect, followed by **Conj1**, while the lowest effect was obtained by **Conj3** even that it contains two drug molecules. **Conj2** showed higher antitumor activity compared to the free Dau.

Comparing the results obtained *in vitro* and *in vivo*, it can be concluded that the position of the drug has a strong influence on the biological activity of the conjugates. Furthermore, the acetylated N-terminus in native α-MSH is important and the modification is not allowed in this position. Based on these results, **Conj2** as lead compound was further modified for the next experiments.

2.3. Biological Characterization of the Sequentially Optimized α-MSH Drug Conjugate, Conj4

Starting from the results obtained by preliminary studies, we optimized the sequence of native α-MSH, focusing on the central region of α-MSH considering literature and experimental data. *In vitro* and *in vivo* measurements were also performed for this newly synthesized and optimized sequence-containing conjugate. In these studies, not only daunomycin but also **Conj2** was used as a positive control.

2.3.1. Experimental Model Selection Based on MC1R Expression

Since MC1R is known to be overexpressed on the surface of cancer cells in a subset of melanoma patients [57], we decided to investigate which melanoma cell lines have a high expression of MC1R. First, we investigated the mRNA expression of MC1R by real-time qPCR (Figure 4) on several cell lines, namely OCM-1, OCM-3, SK-MEL-202, WM983A, WM983B, and A2058. As healthy controls, we used the skin fibroblasts CCD986-Sk, as well as HUVECs. The cell lines exhibited different expression of MC1R, showing the highest in the case of OCM-1. WM983A and OCM-3 also have a relatively high

Preprints (www.preprints.org) | NOT PEER-REVIEWED | Posted: 27 November 2023 doi:10.20944/preprints202311.1667.v1

expression of MC1R, displaying over 10 times elevation compared to healthy controls. Metastatic cell lines such as WM983B, SK-MEL-202, and A2058 did not show highly elevated levels of MC1R mRNA compared to healthy controls.

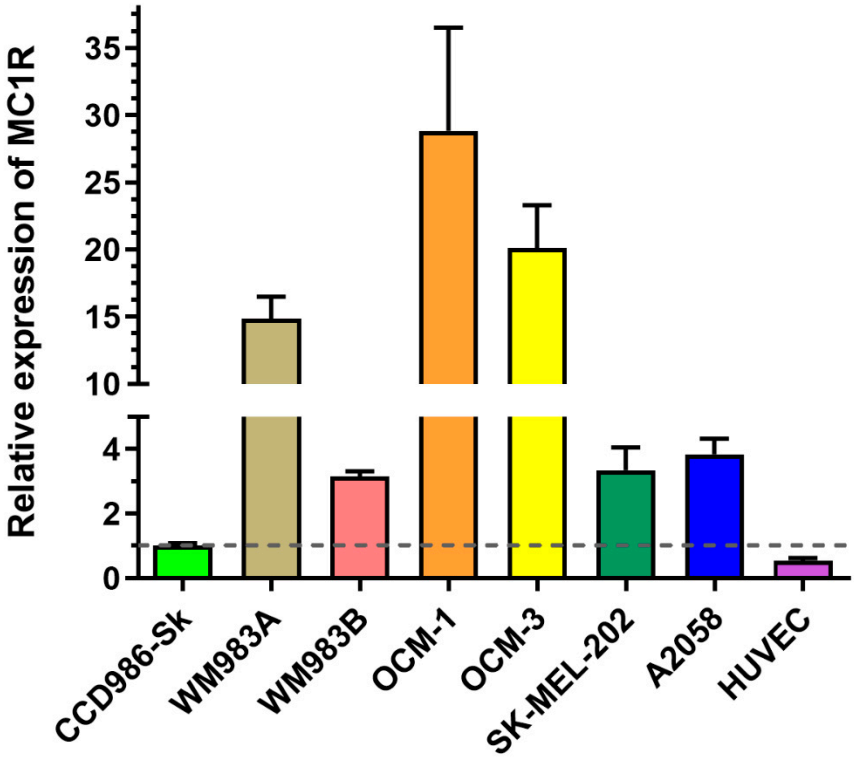

Figure 4. Determination and comparison of mRNA expression level of MC1R by real-time qPCR on different melanoma and healthy control cells. Relative expression was determined by normalizing the expression levels to the healthy skin fibroblast cell line, CCD-986-Sk. The data represents three independent experiments, each performed in 3 technical replicates.

2.3.2. In Vitro Cytostatic Effect of the Conj4 Compared to the Conj2

The *in vitro* cytostatic effect of Dau-α-MSH conjugates was compared by PrestoBlue assay. The same six human melanoma cell lines were used as for the real-time qPCR assay. According to our results, free daunomycin exhibited the lowest IC_{50} values, meaning the highest cytostatic effect which is by the fact that free daunomycin passively diffuses into cells [58,59]. Our Dau-α-MSHs showed similar trends in the effectiveness of the tested cell lines. **Conj2** and **Conj4** resulted in IC_{50} values in the low μM range, (Table 3). When calculating the targeting indices (TI - Table 3) in the case of compound **Conj2**, it could result in over 2 times higher targeting efficiency in most cell lines compared to the A2058 cell line (Table 3). Interestingly, WM983A showed the lowest TI among the high-MC1R-expressing cell lines compared to A2058, and WM983B exhibited great TI regardless of relatively low MC1R expression on the mRNA level. In the case of **Conj4**, the treatment resulted in the highest TIs with OCM-1 and WM983B cell lines.

Preprints (www.preprints.org) | NOT PEER-REVIEWED | Posted: 27 November 2023 doi:10.20944/preprints202311.1667.v1

Table 3. *In vitro* cytostatic effect of the Dau-α-MSH conjugates.

Code	IC_{50} (μM)[1]					
	OCM-1	**OCM-3**	**SK-MEL-202**	**WM983A**	**WM983B**	**A2058**
Free Dau	0.73 ± 0.06	0.56 ± 0.05	0.045 ± 0.12	0.19 ± 0.06	0.33 ± 0.05	0.12 ± 0.07
Conj2	2.51 ± 0.06	2.39 ± 0.06	0.13 ± 0.09	0.79 ± 0.05	1.00 ± 0.00	0.95 ± 0.12
Conj4	29.68 ± 0.06	25.47 ± 0.08	2.06 ± 0.10	13.50 ± 0.06	10.18 ± 0.06	7.15 ± 0.07
	Targeting Index (TI)[2]					
Conj2	2.30	1.85	2.74	1.90	2.61	1.00
Conj4	1.47	1.31	1.30	0.84	1.93	1.00

[1] IC_{50} values were determined by a computerized curve-fitting program (GraphPad Prism 6). Cells were treated with the compounds at 0.003-200 μM concentration range dissolved in the corresponding serum-free medium for 72 h. After the treatment, the PrestoBlue assay was carried out to determine the IC_{50} values. Values shown are mean ± SEM of three independent experiments, each performed in three parallels. [2]TI was determined using the equation of TI=((IC_{50}neg)/(IC_{50}pos)conjugate) / ((IC_{50}neg)/(IC_{50}pos)free drug)).

2.3.3. In Vitro Flow Cytometry and Confocal Microscopy Evaluation

To compare the internalization ability and the intracellular localization of **Conj4** and **Conj2,** flow cytometric and fluorescence microscopic measurements were carried out. First, both conjugates were monitored on the above-mentioned six melanoma cell lines in different concentrations (Figure 5a and 5b). A concentration-dependent cellular uptake profile was observed for both conjugates, but a significant difference in the fluorescence intensity of the conjugates was detected. **Conj2** has significantly higher (4-5-times) fluorescence intensity compared to **Conj4** in all cell lines, except for A2058 where the uptake was lower, but comparable to the other cell lines. The highest uptake levels were detected in the cases of SK-MEL-202, WM983A, and OCM-1. We also monitored the subcellular localization of the internalized conjugates by confocal microscopy (Figure 5c and 5d) First, A2058 cells were used to image the uptake of the conjugates. We could detect the presence of the Dau-α-MSHs in the cytoplasm, partly co-localizing with lysosomes, as well as in nuclei. In the case of this cell line, **Conj4** demonstrated higher uptake compared to **Conj2** and could be detected in a higher amount in the nuclei (that correlates with the flow cytometry data) (Figure 2). In contrast, in the case of OMC-1 cells that showed higher MC1R mRNA expression most of the Dau (probably the active metabolite) could be detected at their target compartment (in the nuclei) both at 12.5 μM and 25 μM concentrations. In line with the flow cytometry data, the signal for **Conj2** was higher compared to **Conj4** (Figure 5d). It is worth mentioning that confocal microscopy images were taken to detect subcellular localization, and not for quantitative measurements. Hence, Dau signals were set during image processing to show similar signal strength to be able to compare localization (at the same settings, **Conj2** was not visible when **Conj4** was set to the level seen in Figure 5d).

Preprints (www.preprints.org) | NOT PEER-REVIEWED | Posted: 27 November 2023 doi:10.20944/preprints202311.1667.v1

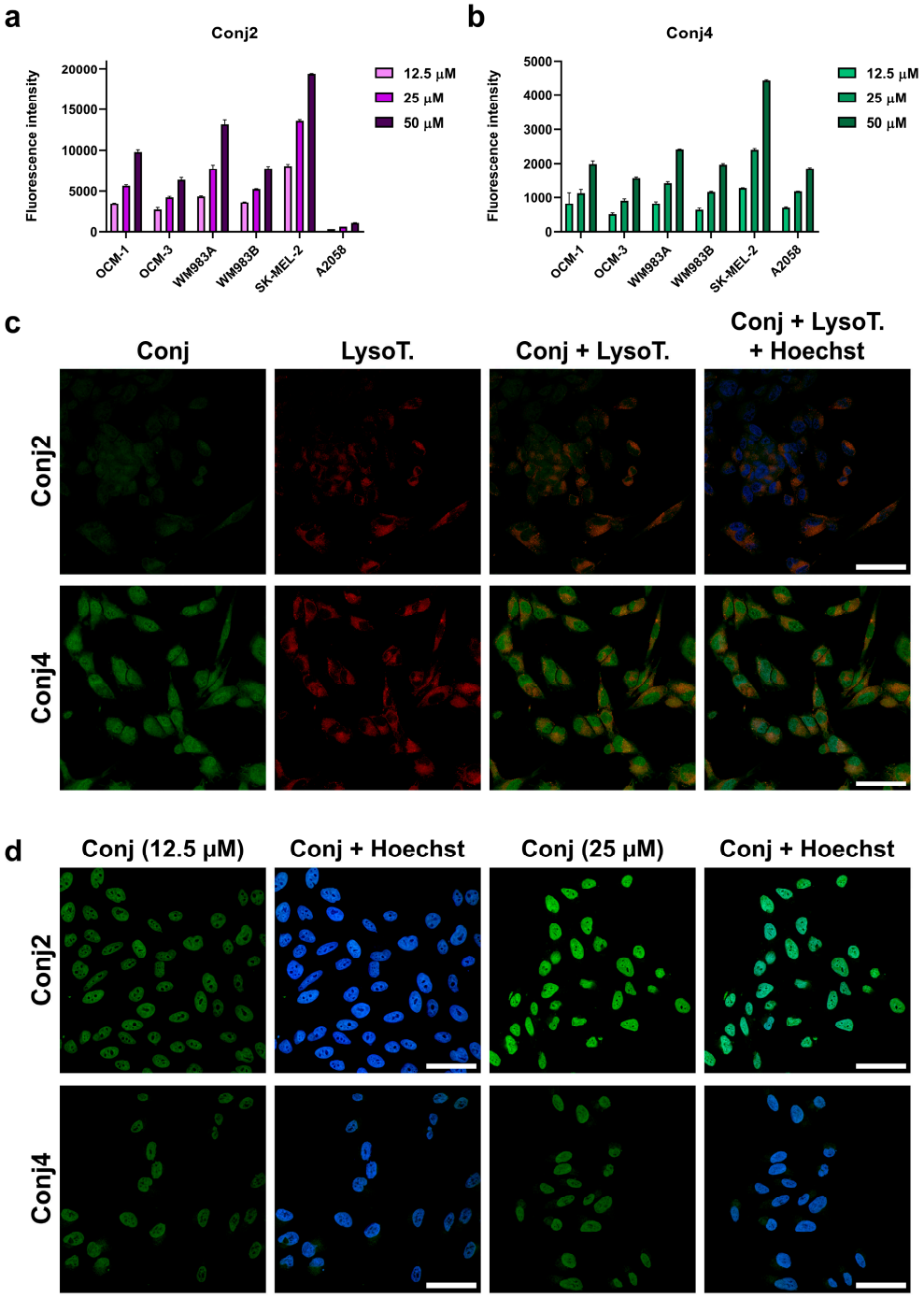

Figure 5. Comparison of cellular uptake profile and subcellular localization of **Conj2** and **Conj4** measured by flow cytometry and confocal microscopy. Comparison of the uptake of **Conj2** (**a**) and **Conj4** (**b**) on different melanoma cells after 3 h by flow cytometry. Subcellular localization of Dau-*α*MSH imaged by confocal microscopy. (**c**) Comparison of uptake of **Conj2** and **Conj4** (green) by A2058 cells after 3 h incubation. Lysosomes were stained with LysoTrackerTM Deep Red (red), nuclei were stained with Hoechst 33342 (blue). (**d**) Localization of uptake of **Conj2** and **Conj4** by OCM-1 cells. Scale bars represent 50 µm.

Considering the above-described results obtained by RT-qPCR, cellular uptake as well as antiproliferative assays, OCM-1, SK-MEL-202 and WM983A cells proved to be the most promising for the establishment of murine experimental *in vivo* models.

Preprints (www.preprints.org) | NOT PEER-REVIEWED | Posted: 27 November 2023 doi:10.20944/preprints202311.1667.v1

2.3.4. In Vivo Experiments

Following the first *in vivo* experiment, the sequence of the native α-MSH was optimized by focusing on the central region of the peptide. The efficacy of the newly designed and synthesized conjugate **Conj4** was tested *in vitro* and further in an *in vivo* experiment to determine the *in vivo* antitumor efficacy of **Conj4** compared to **Conj2** and the free drug (Dau).

With the three best-performing cell lines in the *in vitro* tests, we decided to investigate the tumor establishment and growth abilities in a murine experimental model, which were OCM-1, SK-MEL-202 and WM983A. Cells were inoculated subcutaneously, and tumor progression and general conditions of the mice were monitored. In the case of SK-MEL-202, and WM983A cell lines, a solid tumor was established approximately 12-13 days after inoculation, however, we reported poor tumor growth (Figure 6). On the other hand, OCM-1 cells were able to establish a solid tumor 8 days after injection, and we witnessed exponential tumor growth reaching approximately 2000 mm^3 at day 40. Moreover, the tumor that was established using the OCM-1 cell line grew similarly regardless of the number of cancer cells injected. Since the general fitness of mice decreased in a similar pattern in all models, we decided to choose the OCM-1 cell line to establish our murine model, so that only efficacious Dau-α-MSHs are able to affect the tumor expansion.

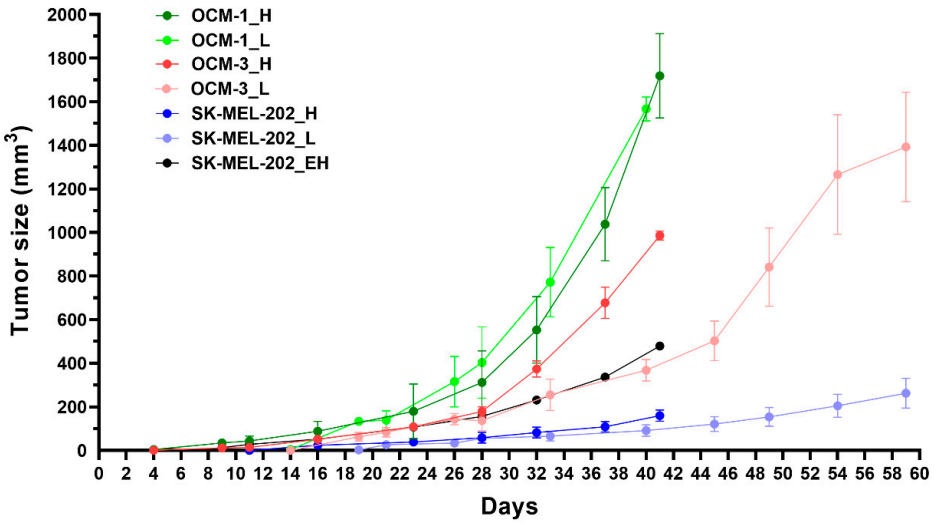

Figure 6. Determination of tumor establishment and growth abilities of the most promising cell lines (OCM-1, SK-MEL-202 and WM983A) in murine experimental model. L: low inoculated cell number (500 000 cells/mice), H: high inoculated cell number (1 000 000 cells/mice), EH: 2 000 000 cells/mice.

When investigating the effect of Dau-α-MSHs and free drug on tumor growth *in vivo*, male NOD-SCID mice were treated three times with saline as a control treatment and with each of the compounds, however, the doses varied based on the maximum tolerated dose (MTD) that was identified prior to the experiment (Figure S6). Mice were treated 1 mg/kg with free drug, 5 mg/kg with **Conj2,** and 10 mg/kg with **Conj4**. Dau-α-MSHs and free drug-treated groups started to separate in tumor size from the control group at day 23. The general condition of free drug-treated mice declined rather fast and on day 28, mice had to be terminated. The rest of the groups were terminated on day 33 since animals including **Conj2**-treated mice reached the cut-off value of weight loss (Figure 7a). At the beginning of the treatment, free daunomycin seemed to be able to keep up with the efficacy of the Dau-αMSHs, on the other hand, it resulted in high toxicity and lack of tumor inhibition compared to control (Figure 7b). On Day 33, the tumor size of **Conj2** treated mice was reduced to 55% of the control size. Moreover, **Conj4** was also able to reduce the tumor size by 14% compared to control, however, this did not seem to be a statistically significant inhibition (Figure 7b).

Preprints (www.preprints.org) | NOT PEER-REVIEWED | Posted: 27 November 2023 doi:10.20944/preprints202311.1667.v1

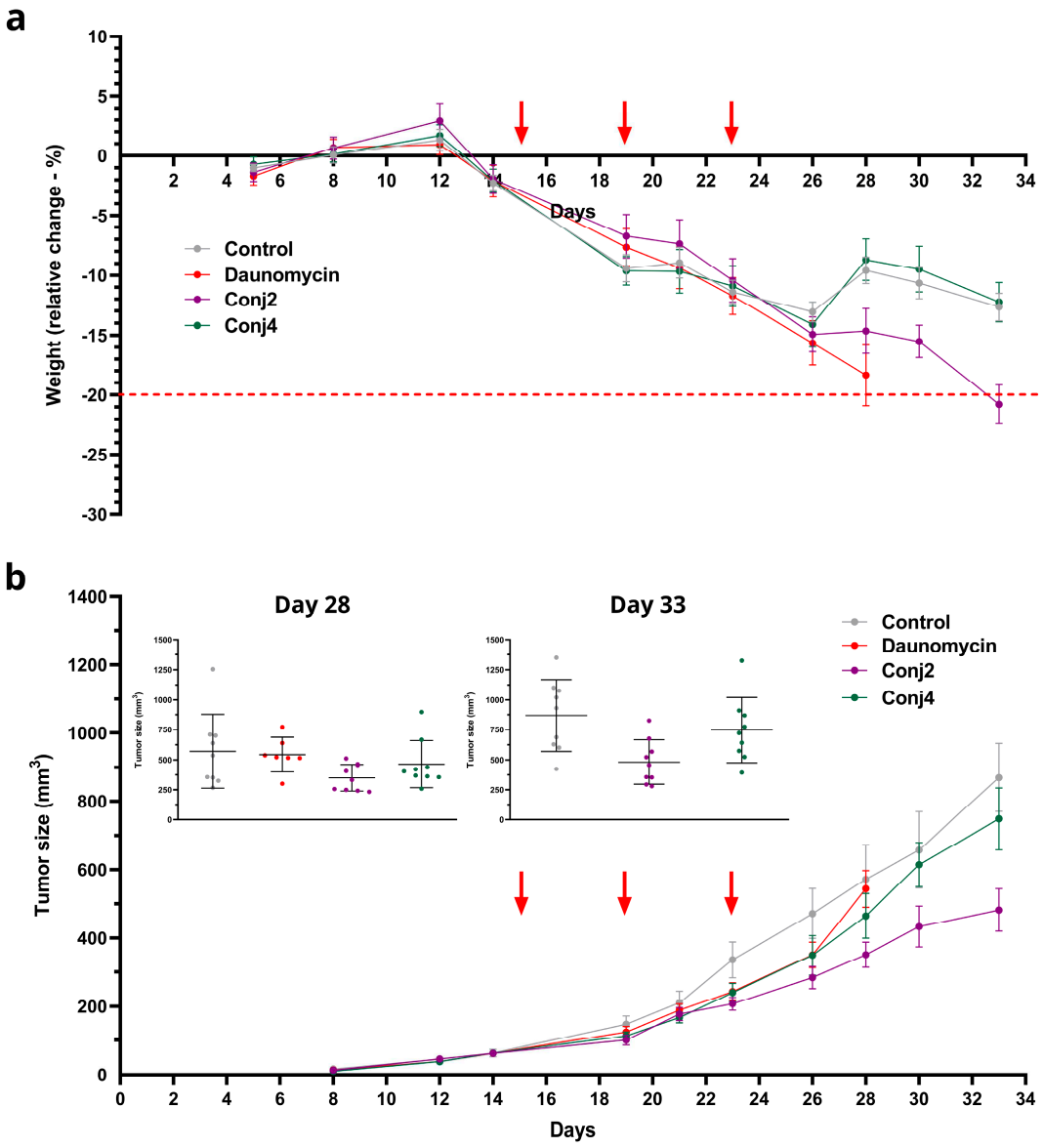

Figure 7. Determination of *in vivo* tumor growth inhibitory effect of **Conj2** and **Conj4** on OCM-1 tumor bearing murine model: (**a**) Body weight of the mice (grams, average ± SEM); (**b**) Tumor volume (mm^3, average ± SEM). 7 animals per group.

3. Discussion

Chemotherapy, which is one of the main approaches for cancer treatment, is mostly ineffective for advanced melanoma due to its high metastatic nature. The failure of this classical treatment requires the development of more effective therapeutic agents and treatment strategies. MC1R overexpression can be detected in over 80% of melanoma patients [57]. This observation allows targeted delivery of drugs using MC1R-specific homing peptides. In this article, we used α-MSH peptide as the ligand of MC1R. Daunomycin as a chemotherapeutic drug molecule was applied in the conjugates. Dau as an auto-fluorescent agent is suitable for the detection of the conjugates in cellular uptake studies both with flow cytometry and confocal microscopy. Therefore, the comparison of conjugates with different homing peptides can be done easily which helps to select the appropriate conjugates for further development. In this study, a non-cleavable oxime linkage was applied for conjugation. We demonstrated in our previous studies, that the oxime bond is stable in circulation and active metabolites can be released in lysosomes. In these metabolites, the Dau is connected to the attached amino acid (Dau=Aoa-Aaa-OH or H-Lys(Dau=Aoa)-OH). These

 doi:10.20944/preprints202311.1667.v1

metabolites can bind to DNA with different binding affinity depending on the type of amino acids (70). Appropriate homing peptide – Dau conjugates show high antitumor effects both *in vitro* and *in vivo*. Because of the low toxicity of such type of conjugates significant tumor growth inhibition could be detected in several tumors *in vivo* that was even higher than the effect of the free drug in the maximum tolerated dose.

In the first experiment, Dau was attached to the full-length α-MSH in which Met was substituted by Nle which is allowed (30, 34, 36) and provides an easier synthesis by avoiding side reactions of Met. The drug was connected either to the N-terminus (**Conj1**) or to the side chain of Lys in position 11 (**Conj2**) or to both (**Conj3**). Despite **Conj1** showing a slightly lower cytostatic effect and entry into different melanoma cells, all of them were investigated *in vivo* as the first screen on aggressive and fast-growing B16 murine melanoma-bearing mice. Interestingly, the conjugates with two drug molecules which showed significant *in vitro* effects did not inhibit the tumor growth at all. In contrast, **Conj2** had significant tumor growth inhibition (ca. 40%) that was higher than the effect of the free Dau in the maximum tolerated doses. **Conj1** was also not active *in vivo*, thus **Conj2** was selected for further development. These data highlights the importance of the binding sites in peptide drug conjugates especially in the case of using non-cleavable spacer. It can be also concluded that the position of the drug in the homing peptide is more important than the number of drugs in the conjugate. Furthermore, it seems that the *in vitro* studies alone are not adequate to conclude the efficiency of peptide-drug conjugates.

In the second experiment, our goal was to identify whether the truncation of the terminal parts of the homing peptide (in **Conj2**) - but at the same time keeping the central sequence (**Conj4**) that has responsibility in receptor binding - is allowed without loss of the biological activity. In **Conj4** the Phe was replaced by its D-isomers which is suggested to increase the receptor binding affinity of α-MSH derivatives [34–36]. In addition, further relevant human melanomas containing MC1R were included into this experiment. The receptor expression level of the cells was determined by RT-qPCR. This shortened conjugate (**Conj4**) showed excellent cellular uptake by A2058 cells and fast localization in the nucleus in comparison with **Conj2**. Surprisingly, its *in vitro* cytostatic effect was ca. on an order of magnitude lower than **Conj2**. It was also detected that the cellular uptake on another type of melanomas preferred **Conj2** suggesting some differences in the uptake mechanism. The lower cytostatic effect of **Conj4** can be explained by the different metabolite that was released upon digestion by Cathepsin B in lysosomes (*e.g.* H-Lys(Dau=Aoa)-NH_2) because of the C-terminal position of the Dau containing lysine residue.

The second *in vivo* experiment was performed on OCM-1, Ocular Choroidal Melanoma-1 bearing mice using **Conj2** and **Conj4**. Choroidal melanoma is a rare malignant tumor, but the second on the list of the top ten most malignant melanoma sites in the body with high metastatic capability (around 50% of choroidal melanoma patients develop metastases) [60]. In our experiment, OCM-1 provided the highest MC1R mRNA level therefore, it seemed relevant to investigate the *in vivo* tumor growth inhibition in this type of melanoma. During the treatments (three injections between days 15 and 23 after tumor inoculation) no significant differences in the activity could be detected. However, mice treated with the free Dau showed significant weight loss representing its toxicity therefore, they had to be terminated on day 28. Without further treatment, in the next days, the tumor growth inhibition was more pronounced by **Conj2** than **Conj4** reaching statistically significant inhibition compared to control animals. This observation suggests that **Conj2** might have a long-term antitumor effect and might be a better candidate for drug development.

4. Materials and Methods

4.1. Materials

The materials applied for the synthesis and conjugation of peptides with their abbreviation are listed in the Supplementary Materials.

 doi:10.20944/preprints202311.1667.v1

4.2. Synthetic Procedures and Chemical Characterization

The α-MSH peptide derivatives (native and truncated ones) were synthesized manually on Rink Amide MBHA resin (0.67 mmol/g capacity) using standard Fmoc/^{t}Bu strategy with DIC-HOBt coupling reagents. However, when Dau was conjugated to the side chain of Lys in position 11, the ε-amino group was protected with a selectively removable Dde-protecting group. At the end of the synthesis of the peptide sequence, the N-terminal Fmoc group was cleaved with 2% piperidine + 2% DBU in DMF (in four steps 2 + 2 + 5 + 10 min), then they were handled differently depending on the type of conjugates. In the case of the synthesis of **Conj2** and **Conj4**, after the N-terminal acetylation (Ac_2O:DIEA:DMF (1:1:3, v/v/v%) the Lys side chain protecting group (Dde) was selectively cleaved with 2% hydrazine hydrate (6x2 min). On the other hand, for the synthesis of two Dau-containing conjugates (**Conj3**), both the Fmoc and the Dde protecting groups were removed, respectively. Boc-Aoa-OH was attached either to the N-terminus and/or to the ε-amino group of the Lys still on the resin using the standard coupling agents.

Peptides were cleaved from the resin with TFA/H_2O/TIS (9.5:2.5:2.5, v/v/v) mixture (2 h, RT). After filtration, compounds were precipitated in cold diethyl ether, centrifuged (4.000 rpm, 5 min), and freeze-dried from water. The crude peptides were characterized before the ligation by analytical RP-HPLC and ESI-HRMS. The crude compound was clean enough and used in the next synthetic step without any purification.

Oxime ligation was performed as described previously (Szabó et al., 2015). Briefly, the aminooxy-functionalized α-MSH peptides were dissolved in 0.2 M NaOAc solution (pH 5.2) and Dau·HCl (10% excess to the peptide) was added to the solution. Oxime ligation was carried out almost quantitatively in a day. The oxime bond-linked Dau–α-MSH conjugates were characterized by analytical RP-HPLC and ESI-HRMS (Figure S1-S4).

4.3. Reverse Phase High-Performance Liquid Chomatography (RP-HPLC)

The purification of crude peptides and conjugates was performed on an UltiMate 3000 Semiprep HPLC (Thermo Fisher Scientific) with a Phenomenex Jupiter Proteo C-12 column (250 × 10 mm) using gradient elution, consisting of 0.1% TFA in water (eluent A) and 0.1% TFA in acetonitrile/water = 80/20 (v/v) (eluent B).

The crude and purified peptides were analyzed by analytical RP-HPLC (Shimadzu prominence HPLC system) with a Phenomenex Jupiter Proteo C-12 column (150 × 4.6 mm) using gradient elution, consisting of 0.1% TFA in water (eluent A) and 0.1% TFA in acetonitrile/water = 80/20 (v/v) (eluent B).

4.4. Electrospray Ionization-High-Resolution Mass Spectromerty (ESI-HRMS)

The identification of the products was achieved by high-resolution mass spectrometry using Thermo Scientific Q Exactive Focus Hybrid Quadrupole-Orbitrap Mass Spectrometer. Samples were dissolved in 50% acetonitrile - 50% water containing 0.1% formic acid. Mass spectra were recorded in positive mode in the m/z 200-1500 range.

4.5. Cell Culturing

The following cell cultures were used for biological evaluation of the synthetic melanoma-specific peptide-drug (Dau-α-MSH) conjugates: A2058 (human skin melanoma, CVCL_1059), M24 (human metastatic skin melanoma, CVCL_D032), OCM-1 (human Ocular Choroidal Melanoma-1, CVCL_6934), OCM-3 (human Ocular Choroidal Melanoma-3, CVCL_6937), WM983A (human metastatic skin melanoma, CVCL_6808), WM983B (human metastatic skin melanoma CVCL_6809), SK-MEL-202 (human skin melanoma, ATCC HTB-68) and B16 (mouse melanoma, ATCC: CRL-6475). Cells were maintained in RPMI-1640 (Lonza, Basel, Switzerland), supplied with 10% FBS (fetal bovine serum; BioSera, Nuaille, France), L-glutamine, and 1% penicillin–streptomycin (from 10 000 units penicillin and 10 mg streptomycin/mL, Gibco, Dublin, Ireland) at 37 °C in a 5% CO_2 atmosphere. No mycoplasma contamination was detected in the cell cultures.

 doi:10.20944/preprints202311.1667.v1

4.6. Determination of mRNA Expression Level of Melanoma Cells by qPCR

The relative RNA expression of MC1R gene was determined using the RT-qPCR method. The total RNA from the investigated cell lines was isolated using Trizol® reagent (Ambion, by Life Technologies, Carlsbad, CA, USA). The concentration and the quality of the RNA samples obtained were measured using a spectrophotometer (NanoDrop ND-1000, Wilmington, DE, USA) at an absorbance of 260 nm and 280 nm. The cDNA synthesis was completed in Eppendorf 5331 Mastercycler Gradient thermocycler (Eppendorf, Enfield, CT, USA). 500 ng of total RNA was transcribed into cDNA according to the protocol of the Reverse Transcription System provided by Promega (Promega, Madison, Wisconsin, USA). Afterwards, the cDNA samples were stored at -20 °C until further processing. The primers were obtained from Sigma-Aldrich, St. Louis, Missouri, USA, and were designed based on the reference sequence obtained from NCBI RefSeq (NM_002386.4). Primer sequences are as follows: MC1R_forward - CATCGCCGTGGACCGCTACATC, MC1R_reverse - GCTGAAGACGACACTGGCCACC. Relative expression of MC1R was measured using SsoAdvanced Universal SYBR® Green Supermix assay (Bio-Rad, Hercules, California, USA) with a CFX96 Touch Real-Time PCR Detection System (Bio-Rad, Hercules, California, USA). Relative expression was determined by normalizing the expression levels to the healthy skin fibroblast cell line, CCD-986-Sk. The data represents three independent experiments, each performed in 3 technical replicates.

4.7. Determination of the In Vitro Antiproliferative Activity

The *in vitro* cytostatic effect of Dau-α-MSH conjugates was determined by two different assays. The full-length Dau-α-MSH conjugates were investigated by MTT assay [61–65] using human and murine melanoma cell cultures. For determination of the cytostatic effect of these conjugates, the cells were treated with the compounds at 0.8-100 µM concentration range dissolved in the corresponding serum-free media for 24 h. After incubation, the treating solutions were removed, the cells were washed two times with serum-free medium and cultured for 48 h in the appropriate serum-containing cell culture medium. On the fourth day, the MTT assay was carried out to determine the IC_{50} values of the compounds. IC_{50} is the concentration that inhibits cell proliferation by 50%. Statistical analysis of the MTT's data was performed by Student's t-test of Origin®2018 at the 95% confidence level.

The *in vitro* cytostatic effect of Dau-α-MSH conjugate with optimized sequence (**Conj4**) was investigated and compared with **Conj2** by PrestoBlue assay [66–68] using human melanoma cell cultures with different origins. For determination of the cytostatic effect of the conjugates, the cells were treated with the compounds at 0.003-200 µM concentration range dissolved in the corresponding serum-free medium for 72 h. After the treatment, the PrestoBlue assay (purchased from Invitrogen (Waltham, Massachusetts, USA) was carried out to determine the IC_{50} values of the compounds. Based on the IC_{50} values, we also determined the targeting index (TI) of the conjugates using the following equation [69]:

$$TI = \frac{\left(\frac{IC50neg}{IC50pos}\right) conjugate}{\left(\frac{IC50neg}{IC50pos}\right) free\ drug}$$

4.8. In Vitro Flow Cytometry Evaluation

The human melanoma cell cultures with different origins were cultured as described above. To study the cellular uptake of the Dau-α-MSH conjugates, 10^5 cells per well were plated on 24-well plates one day prior to the experiment. After 24 h incubation at 37°C, cells were treated for 3 h with the compounds solved in the corresponding serum-free medium. The cellular uptake of the compounds was investigated in the 12.5-50 µM concentration range. Cells treated with serum-free medium for 3 h were used as a control. After incubation, the medium was removed, and the cells

 doi:10.20944/preprints202311.1667.v1

were treated with 100 µl trypsin for 10 min. Trypsin digestion was stopped by the addition of 900 µl HPMI medium (9 mM glucose, 10 mM $NaHCO_3$, 119 mM NaCl, 9 mM (4-(2-hydroxyethyl)-1-piperazineethanesulfonic acid (HEPES), 5 mM KCl, 0.85 mM $MgCl_2$, 0.053 mM $CaCl_2$, 5 mM $Na_2HPO_4 \times 2H_2O$, and pH 7.4) containing 10% FBS, and the cells were moved from the plate to FACS tubes. Cells were centrifuged at 216 g at 4°C for 5 min and the supernatant was removed. After this procedure, cells were resuspended in 250 µl HPMI, and the increase of the fluorescence intensity of different types of melanoma cells was monitored by flow cytometry (BD LSR II, BD Bioscience, San Jose, CA). Data was analyzed with FACSDiVa 5.0 software.

4.9. Immunostaining and Confocal Microscopy

A2058 and OCM-1 cells were seeded to coverslip-containing (thickness 1, Assistant, Karl Hecht GmbH & Co KG, Sondheim/Rhön, Germany) 24-well plates (Sarstedt, Nümbrecht, Germany) one day prior to treatment at a density of $5 \cdot 10^4$ cells/well. Cells were treated with 12.5 and 25 µM of Dau-α-MSH conjugates that were diluted in a serum-free medium for 3 h. Lysosomes were stained with LysoTracker™ Deep Red (Thermo Fisher Scientific, Waltham, MA, USA, 300 nM for 30 min, followed by nucleus staining with Hoechst 33342 (0.2 µg/ml, 10 min). After washing with phosphate-buffered saline (PBS, Lonza, Basel, Switzerland), cells were fixed with 4% paraformaldehyde for 20 min at 37°C. Coverslips were mounted to microscopy slides by Mowiol® 4–88 mounting medium (Sigma-Aldrich, St. Louis, Missouri, USA). Confocal microscopy images were acquired on a Zeiss LSM 710 (in case of A2058 cells) or Zeiss LSM 780 confocal microscope (in case of OCM-1 cells) (Carl Zeiss Microscopy GmbH, Jena, Germany) using a Plan-Apochromat 40x/1.4 Oil DIC M27 objective. Hoechst 33342 and daunomycin-conjugates and LysoTracker Deep Red were excited with lasers 405, 488 and 633 nm, respectively. ZEN Lite (Carl Zeiss Microscopy GmbH) software was used for image processing.

4.10. Experimental Animals

Different murine models were used for *in vivo* experiments. For determination of *in vivo* toxicity as well as for *in vivo* antitumor activity of the drug and the conjugates, adult male BALB/c, C57BL/6 or NOD-SCID mice were used. Mice were kept in a sterile environment in Makrolon® cages at 22–24°C (40–50% humidity), with light regulation of 12/12 h light/dark. The animals had free access to sterilized tap water and were fed a sterilized standard diet (VRF1, autoclavable, Akronom Kft., Budapest, Hungary) *ad libitum*. Animals used in our study were taken care of according to the "Guiding Principles for the Care and Use of Animals" based on the Helsinki declaration, and they were approved by the ethical committee of the National Institute of Oncology. Animal housing density was according to the regulations and recommendations from directive 2010/63/EU of the European Parliament and of the Council of the European Union on the protection of animals used for scientific purposes. Permission license for breeding and performing experiments with laboratory animals: PEI/001/1738-3/2015 and PE/EA/1461-7/2020.

4.11. Acute Toxicity Study of Drug, Conj2 and Conj4

To determine toxicity of conjugates on healthy animals, *in vivo* acute toxicity study of Dau, **Conj2** and **Conj4** was performed. In the first experiment, adult BALB/c male mice (29-31 g) were exposed by one injection of the conjugate at the start of experiment, by intraperitoneal (*i.p.*) administration. A dose of 25 mg Dau content/kg was used, in a volume of 0.1 mL per mice (3 mice per condition). In the second *in vivo* experiment, NOD-SCID mice were exposed by four injections of the conjugates at the start of experiment, by intraperitoneal (*i.p.*) administration. A dose of 5, 10 and 15 mg Dau content/kg was used for the toxicity assay, in a volume of 0.1 mL per mice (3 mice per condition). The animals were kept under the conditions as described above.

 doi:10.20944/preprints202311.1667.v1

4.12. In Vivo Antitumor effect of Drug, Conj2 and Conj4

In the first experiment, B16 murine melanoma cells were subcutaneously (*s.c.*) injected into side of the lateroabdominal region of 35 C57BL/6 male mice (20-28 g), which murine strain is syngeneic for the B16 melanoma tumor cell line [70,71], $6.5 \cdot 10^5$ cells in a volume of 200 µl M199 medium was inoculated per animal. The treatment started 9 days after cell inoculation when average tumor volume was 30 mm^3. Compounds were dissolved in saline solution (Teva, Debrecen, Hungary), and administered *via i.p.* injection in a volume of 0.1 mL per 10 g of body weight. 5 groups by 7 animals were established and treated with the following doses and schedule: the mice in the control group were treated with the solvent; free daunomycin (Dau) treated group (1 mg/kg, treatments on days 9 and 17); groups treated with **Conj1**, **Conj2,** and **Conj3** (10 mg/kg Dau content, treatments on days 9, 13, 15, 17 after cell inoculation). Animal weight and tumor volumes were measured initially when the treatment started and at periodic intervals following treatment. A digital caliper was used to measure the longest (a) and the shortest diameter (b) of a given tumor. The tumor volume was calculated using the formula $V = ab^2 \times \pi/6$, whereby a and b represent the measured parameters (length and width). Termination of the experiment was 20 days after cell inoculation, *i.e.* 12 days after treatment started, since the average volume of the tumors in the control group reached over 1800 mm^3. The mice from all groups were sacrificed by cervical dislocation after which their tumors were harvested and weighed for antitumor effect assessment. Antitumor effect of treatments was evaluated measuring the tumor volume and calculating the percentage of how much the tumor volume grew in comparison to the starting tumor volume which was set arbitrarily for all tumors as 100% at the start of treatment.

In the next experiment, firstly the murine xenograft melanoma model establishment studies were performed using 8-12-week-old male NOD-SCID mice. For selection of the most suitable tumor model, three cell lines were inoculated subcutaneously, OCM-1, SK-MEL-202, and WM983A. Cells were injected in 0.1 mL RPMI-1640 basic medium in a concentration of $1.5 \cdot 10^6$ cells/mL, and the tumor growth and weight of mice were monitored 2-3 times per week. Subsequently, the antitumor effects of Dau-α-MSHs were determined in a mouse xenograft melanoma model selected as described above. Once the tumor volume reached 60 mm^3, mice were randomized and assigned to different groups for each treatment: 0.9% saline as a control, free daunomycin, **Conj2** and **Conj4**. Treatments were injected intraperitoneally every fifth day, three times in total (daunomycin dosage of 5 mg/kg in case of **Conj2**, 10 mg/kg for **Conj4**, respectively which was determined based on the toxicity tests, and 1 mg/kg were used for free drug – MTD). The weight and tumor size of mice were monitored during the whole experiment. On Day 33, mice were euthanized, and primary tumor, heart, lung, liver, and spleen were harvested and stored in 4% formalin (Molar Chemicals, Halásztelek, Hungary). In the case of the in vivo allograft model, statistical analyses were performed by GraphPad Prism 6 (GraphPad Software, San Diego, CA, USA) using the non-parametric Mann–Whitney test, where p-values lower or equal than 0.05 were considered statistically significant.

5. Conclusions

In conclusion, we have found that α-MSH derivative SYSNleEHFRWGKPV might be a good homing peptide for MC1R-specific drug targeting, and the side chain of Lys might be a better conjugation site to attach drug molecules to, especially in the case of applying non-cleavable spacers. In this study it was also demonstrated that Ac-SYSNleEHFRWGK(Dau=Aoa)PV-NH_2 conjugate is effective on OCM-1 uveal melanoma therefore, this structure might be a good candidate for further drug development.

Supplementary Materials: The following supporting information can be downloaded at the website of this paper posted on Preprints.org. Figure S1: RP-HPLC chromatogram (a) and ESI-HRMS spectrum (b) of Conj1;Figure S2: RP-HPLC chromatogram (a) and ESI-HRMS spectrum (b) of Conj2; Figure S3: RP-HPLC chromatogram (**a**) and ESI-HRMS spectrum (**b**) of Conj3; Figure S4: RP-HPLC chromatogram (**a**) and ESI-HRMS spectrum (**b**) of Conj4; Figure S5: Acute toxicity of Conj2 on healthy male BALB/c mice; Figure S6: Determination of in vivo toxicity of Conj2 and Conj4 in OCM-1 bearing male NOD-SCID mice; Table S1: Effect of Dau-

conjugates (10 mg Dau content/kg) and free Dau (1 mg /kg) in subcutaneous B16 murine melanoma bearing C57BL/6 male mice in vivo.

Author Contributions: Conceptualization, ISz and GM; methodology: ISz, SzB, JT, BV, GM; formal analysis: ISz, BV, DM, BBK, IR; investigation: ISz, BV, DM, BBK, IR; writing—ISz, BV, DM, BBK, IR; writing—review and editing, ISz, SzB, JT, GM; visualization, BBK, BV, IR, ISz; supervision, ISz, GM; project administration: ISz, GM; funding acquisition: ISz, GM, JT. All authors have read and agreed to the published version of the manuscript.

Funding: The research was funded by the National Research, Development and Innovation Office (NVKP_16-1-2016-0036), the National Laboratories Excellence program (under the National Tumor Biology Laboratory Project (2022-2.1.1-NL-2022-00010)) and the Hungarian Thematic Excellence Program (TKP2021-EGA-44). This work was also supported by grants from European Union's Horizon 2020 research and innovation program under the Marie Skłodowska-Curie grant agreement No 861316 Magic Bullet: reloaded. GH tanks for the financial support of TKP2021-EGA-20 (GH) project that has been implemented with the support provided by the National Research, Development and Innovation Fund of Hungary, financed under the TKP2021-EGA funding scheme. ISz thanks theNew National Excellence Program Bolyai+ (ÚNKP-22-5-ELTE-1157 and ÚNKP-23-5-ELTE-494).

Institutional Review Board Statement: Animals used in our study were taken care of according to the "Guiding Principles for the Care and Use of Animals" based on the Helsinki declaration, and they were approved by the ethical committee of the National Institute of Oncology. Animal housing density was according to the regulations and recommendations from directive 2010/63/EU of the European Parliament and of the Council of the European Union on the protection of animals used for scientific purposes. Permission license for breeding and performing experiments with laboratory animals: PEI/001/1738-3/2015 and PE/EA/1461-7/2020.

Data Availability Statement: We encourage all authors of articles published in MDPI journals to share their research data. In this section, please provide details regarding where data supporting reported results can be found, including links to publicly archived datasets analyzed or generated during the study. Where no new data were created, or where data is unavailable due to privacy or ethical restrictions, a statement is still required. Suggested Data Availability Statements are available in section "MDPI Research Data Policies" at https://www.mdpi.com/ethics.

Acknowledgments: ISz thanks for the János Bolyai research grant of the Hungarian Academy of Sciences (BO/00381/22) and the New National Excellence Program Bolyai+ (ÚNKP-22-5-ELTE-1157 and ÚNKP-23-5-ELTE-494).

Conflicts of Interest: The authors declare no conflict of interest.

References

1. Sung, H.; Ferlay, J.; Siegel, R.L.; Laversanne, M.; Soerjomataram, I.; Jemal, A.; Bray, F. Global Cancer Statistics 2020: GLOBOCAN Estimates of Incidence and Mortality Worldwide for 36 Cancers in 185 Countries. *CA Cancer J Clin* **2021**, *71*, doi:10.3322/caac.21660.
2. Eggermont, A.M.; Spatz, A.; Robert, C. Cutaneous Melanoma. *The Lancet* **2014**, *383*, 816–827, doi:10.1016/S0140-6736(13)60802-8.
3. Clark, W.H.; From, L.; Bernardino, E.A.; Mihm, M.C. The Histogenesis and Biologic Behavior of Primary Human Malignant Melanomas of the Skin. *Cancer Res* **1969**, *29*, 705–727.
4. Helmbach, H.; Rossmann, E.; Kern, M.A.; Schadendorf, D. Drug-Resistance in Human Melanoma. *Int J Cancer* **2001**, *93*, 617–622, doi:10.1002/ijc.1378.
5. Yang, A.S.; Chapman, P.B. The History and Future of Chemotherapy for Melanoma. *Hematol Oncol Clin North Am* **2009**, *23*, 583–597, doi:10.1016/j.hoc.2009.03.006.
6. Mishra, H.; Mishra, P.K.; Ekielski, A.; Jaggi, M.; Iqbal, Z.; Talegaonkar, S. Melanoma Treatment: From Conventional to Nanotechnology. *J Cancer Res Clin Oncol* **2018**, *144*, 2283–2302, doi:10.1007/s00432-018-2726-1.
7. Patel, P.M.; Suciu, S.; Mortier, L.; Kruit, W.H.; Robert, C.; Schadendorf, D.; Trefzer, U.; Punt, C.J.A.; Dummer, R.; Davidson, N.; et al. Extended Schedule, Escalated Dose Temozolomide versus Dacarbazine in Stage IV Melanoma: Final Results of a Randomised Phase III Study (EORTC 18032). *Eur J Cancer* **2011**, *47*, 1476–1483, doi:10.1016/j.ejca.2011.04.030.
8. Chiarion-Sileni, V.; Guida, M.; Ridolfi, R.; Romanini, A.; Brugnara, S.; Del Bianco, P.; Perfetti, E.; Cavallo, R.; Pigozzo, J.; Donati, D.; et al. Temozolomide (TMZ) as Prophylaxis for Melanoma Brain Metastases (BrM):

Results from a Phase III, Multicenter Study. *Journal of Clinical Oncology* **2008**, *26*, 20014–20014, doi:10.1200/jco.2008.26.15_suppl.20014.

9. Friedman, R.J.; Rigel, D.S.; Kopf, A.W. Early Detection of Malignant Melanoma: The Role of Physician Examination and Self-Examination of the Skin. *CA Cancer J Clin* **1985**, *35*, 130–151, doi:10.3322/canjclin.35.3.130.
10. Lee, C.; Collichio, F.; Ollila, D.; Moschos, S. Historical Review of Melanoma Treatment and Outcomes. *Clin Dermatol* **2013**, *31*, 141–147, doi:10.1016/j.clindermatol.2012.08.015.
11. Rebecca, V.W.; Sondak, V.K.; Smalley, K.S.M. A Brief History of Melanoma. *Melanoma Res* **2012**, *22*, 114–122, doi:10.1097/CMR.0b013e328351fa4d.
12. Gerstenblith, M.R.; Goldstein, A.M.; Fargnoli, M.C.; Peris, K.; Landi, M.T. Comprehensive Evaluation of Allele Frequency Differences of *MC1R* Variants across Populations. *Hum Mutat* **2007**, *28*, 495–505, doi:10.1002/humu.20476.
13. Beaumont, K.A.; Shekar, S.L.; Newton, R.A.; James, M.R.; Stow, J.L.; Duffy, D.L.; Sturm, R.A. Receptor Function, Dominant Negative Activity and Phenotype Correlations for MC1R Variant Alleles. *Hum Mol Genet* **2007**, *16*, 2249–2260, doi:10.1093/hmg/ddm177.
14. Schiöth, H.B.; Phillips, S.R.; Rudzish, R.; Birch-Machin, M.A.; Wikberg, J.E.S.; Rees, J.L. Loss of Function Mutations of the Human Melanocortin 1 Receptor Are Common and Are Associated with Red Hair. *Biochem Biophys Res Commun* **1999**, *260*, 488–491, doi:10.1006/bbrc.1999.0935.
15. Fernandez, L.; Milne, R.; Bravo, J.; Lopez, J.; Avilés, J.; Longo, M.; Benítez, J.; Lázaro, P.; Ribas, G. MC1R: Three Novel Variants Identified in a Malignant Melanoma Association Study in the Spanish Population. *Carcinogenesis* **2007**, *28*, 1659–1664, doi:10.1093/carcin/bgm084.
16. Ichii-Jones, F.; Yengi, L.; Bath, J.; Fryer, A.A.; Strange, R.C.; Lear, J.T.; Heagerty, A.H.M.; Smith, A.G.; Hutchinson, P.E.; Osborne, J.; et al. Susceptibility to Melanoma: Influence of Skin Type and Polymorphism in the Melanocyte Stimulating Hormone Receptor Gene. *Journal of Investigative Dermatology* **1998**, *111*, 218–221, doi:10.1046/j.1523-1747.1998.00287.x.
17. Kennedy, C.; ter Huurne, J.; Berkhout, M.; Gruis, N.; Bastiaens, M.; Bergman, W.; Willemze, R.; Bouwes Bavinck, J.N. Melanocortin 1 Receptor (MC1R) Gene Variants Are Associated with an Increased Risk for Cutaneous Melanoma Which Is Largely Independent of Skin Type and Hair Color. *Journal of Investigative Dermatology* **2001**, *117*, 294–300, doi:10.1046/j.0022-202x.2001.01421.x.
18. Landi, M.T.; Kanetsky, P.A.; Tsang, S.; Gold, B.; Munroe, D.; Rebbeck, T.; Swoyer, J.; Ter-Minassian, M.; Hedayati, M.; Grossman, L.; et al. MC1R, ASIP, and DNA Repair in Sporadic and Familial Melanoma in a Mediterranean Population. *JNCI: Journal of the National Cancer Institute* **2005**, *97*, 998–1007, doi:10.1093/jnci/dji176.
19. Matichard, E. Melanocortin 1 Receptor (MC1R) Gene Variants May Increase the Risk of Melanoma in France Independently of Clinical Risk Factors and UV Exposure. *J Med Genet* **2004**, *41*, 13e–113, doi:10.1136/jmg.2003.011536.
20. Palmer, J.S.; Duffy, D.L.; Box, N.F.; Aitken, J.F.; O'Gorman, L.E.; Green, A.C.; Hayward, N.K.; Martin, N.G.; Sturm, R.A. Melanocortin-1 Receptor Polymorphisms and Risk of Melanoma: Is the Association Explained Solely by Pigmentation Phenotype? *The American Journal of Human Genetics* **2000**, *66*, 176–186, doi:10.1086/302711.
21. Raimondi, S.; Sera, F.; Gandini, S.; Iodice, S.; Caini, S.; Maisonneuve, P.; Fargnoli, M.C. MC1R Variants, Melanoma and Red Hair Color Phenotype: A Meta-Analysis. *Int J Cancer* **2008**, *122*, 2753–2760, doi:10.1002/ijc.23396.
22. Stratigos, A.J.; Dimisianos, G.; Nikolaou, V.; Poulou, M.; Sypsa, V.; Stefanaki, I.; Papadopoulos, O.; Polydorou, D.; Plaka, M.; Christofidou, E.; et al. Melanocortin Receptor-1 Gene Polymorphisms and the Risk of Cutaneous Melanoma in a Low-Risk Southern European Population. *Journal of Investigative Dermatology* **2006**, *126*, 1842–1849, doi:10.1038/sj.jid.5700292.
23. Valverde, P. The Asp84Glu Variant of the Melanocortin 1 Receptor (MC1R) Is Associated with Melanoma. *Hum Mol Genet* **1996**, *5*, 1663–1666, doi:10.1093/hmg/5.10.1663.
24. van der Velden, P.A.; Sandkuijl, L.A.; Bergman, W.; Pavel, S.; van Mourik, L.; Frants, R.R.; Gruis, N.A. Melanocortin-1 Receptor Variant R151C Modifies Melanoma Risk in Dutch Families with Melanoma. *The American Journal of Human Genetics* **2001**, *69*, 774–779, doi:10.1086/323411.

25. Eberle, A.N.; Rout, B.; Bigliardi Qi, M.; L. Bigliardi, P. Synthetic Peptide Drugs for Targeting Skin Cancer: Malignant Melanoma and Melanotic Lesions. *Curr Med Chem* **2017**, *24*, 1797–1826, doi:10.2174/0929867324666170605105942.
26. Eberle, A.N.; Siegrist, W.; Bagutti, C.; Tapia, J.C.-D.; Solca, F.; Wikberg, J.E.S.; Chhajlani, V. Receptors for Melanocyte-Stimulating Hormone on Melanoma Cells. *Ann N Y Acad Sci* **1993**, *680*, 320–341, doi:10.1111/j.1749-6632.1993.tb19693.x.
27. Jiang, J.; Sharma, S.D.; Fink, J.L.; Hadley, M.E.; Hruby, V.J. Melanotropic Peptide Receptors: Membrane Markers of Human Melanoma Cells. *Exp Dermatol* **1996**, *5*, 325–333, doi:10.1111/j.1600-0625.1996.tb00136.x.
28. Salazar-Onfray, F.; López, M.; Lundqvist, A.; Aguirre, A.; Escobar, A.; Serrano, A.; Korenblit, C.; Petersson, M.; Chhajlani, V.; Larsson, O.; et al. Tissue Distribution and Differential Expression of Melanocortin 1 Receptor, a Malignant Melanoma Marker. *Br J Cancer* **2002**, *87*, 414–422, doi:10.1038/sj.bjc.6600441.
29. Siegrist, W.; Stutz, S.; Eberle, A.N. Homologous and Heterologous Regulation of Alpha-Melanocyte-Stimulating Hormone Receptors in Human and Mouse Melanoma Cell Lines. *Cancer Res* **1994**, *54*, 2604–2610.
30. Hruby, V.J.; Sharma, S.D.; Toth, K.; Jaw, J.Y.; Al-Obeidi, F.; Sawyer, T.K.; Hadley, M.E. Design, Synthesis, and Conformation of Superpotent and Prolonged Acting Melanotropins. *Ann N Y Acad Sci* **1993**, *680*, 51–63, doi:10.1111/j.1749-6632.1993.tb19674.x.
31. Siegrist, W.; Solca, F.; Stutz, S.; Giuffrè, L.; Carrel, S.; Girard, J.; Eberle, A.N. Characterization of Receptors for Alpha-Melanocyte-Stimulating Hormone on Human Melanoma Cells. *Cancer Res* **1989**, *49*, 6352–6358.
32. Miao, Y.; Hylarides, M.; Fisher, D.R.; Shelton, T.; Moore, H.; Wester, D.W.; Fritzberg, A.R.; Winkelmann, C.T.; Hoffman, T.; Quinn, T.P. Melanoma Therapy via Peptide-Targeted α-Radiation. *Clinical Cancer Research* **2005**, *11*, 5616–5621, doi:10.1158/1078-0432.CCR-05-0619.
33. Michael F. Giblin; Nannan Wang; Timothy J. Hoffman; Silvia S. Jurisson; Thomas P. Quinn Design and Characterization of α-Melanotropin Peptide Analogs Cyclized through Rhenium and Technetium Metal Coordination. *PNAS* **1998**, *95*, 12814–12818.
34. Cone, R.D.; Mountjoy, K.G.; Robbins, L.S.; Nadeau, J.H.; Johnson, K.R.; Roselli-Rehfuss, L.; Mortrud, M.T. Cloning and Functional Characterization of a Family of Receptors for the Melanotropic Peptides. *Ann N Y Acad Sci* **1993**, *680*, 342–363, doi:10.1111/j.1749-6632.1993.tb19694.x.
35. Morandini, R.; Suli-Vargha, H.; Libert, A.; Loir, B.; Botyánszki, J.; Medzihradszky, K.; Ghanem, G. Receptor-Mediated Cyotoxicity of a-MSH Fragments Containing Melphalan in a Human Melanoma Cell Line. *Int J Cancer* **1994**, *56*, 129–133, doi:10.1002/ijc.2910560123.
36. Sawyer, T.K.; Sanfilippo, P.J.; Hruby, V.J.; Engel, M.H.; Heward, C.B.; Burnett, J.B.; Hadley, M.E. 4-Norleucine, 7-D-Phenylalanine-Alpha-Melanocyte-Stimulating Hormone: A Highly Potent Alpha-Melanotropin with Ultralong Biological Activity. *Proceedings of the National Academy of Sciences* **1980**, *77*, 5754–5758, doi:10.1073/pnas.77.10.5754.
37. Guo, H.; Yang, J.; Gallazzi, F.; Miao, Y. Effects of the Amino Acid Linkers on the Melanoma-Targeting and Pharmacokinetic Properties of ^{111} In-Labeled Lactam Bridge–Cyclized α-MSH Peptides. *Journal of Nuclear Medicine* **2011**, *52*, 608–616, doi:10.2967/jnumed.110.086009.
38. Lin, X.; Xie, J.; Niu, G.; Zhang, F.; Gao, H.; Yang, M.; Quan, Q.; Aronova, M.A.; Zhang, G.; Lee, S.; et al. Chimeric Ferritin Nanocages for Multiple Function Loading and Multimodal Imaging. *Nano Lett* **2011**, *11*, 814–819, doi:10.1021/nl104141g.
39. Süli-Vargha, H.; Botyánszki, J.; Medzihradszky-Schweiger, H.; Medzihradszky, K. Synthesis of α-MSH Fragments Containing Phenylalanine Mustard for Receptor Studies. *Int J Pept Protein Res* **1990**, *36*, 308–315, doi:10.1111/j.1399-3011.1990.tb00984.x.
40. Sylvie Froidevaux; Martine Calame-Christe; Heidi Tanner; Alex N. Eberle Melanoma Targeting with DOTA-α-Melanocyte-Stimulating Hormone Analogs: Structural Parameters Affecting Tumor Uptake and Kidney Uptake. *Journal of Nuclear Medicine* **2005**, *46*, 887–895.
41. Uchida, M.; Flenniken, M.L.; Allen, M.; Willits, D.A.; Crowley, B.E.; Brumfield, S.; Willis, A.F.; Jackiw, L.; Jutila, M.; Young, M.J.; et al. Targeting of Cancer Cells with Ferrimagnetic Ferritin Cage Nanoparticles. *J Am Chem Soc* **2006**, *128*, 16626–16633, doi:10.1021/ja0655690.
42. Vannucci, L.; Falvo, E.; Fornara, M.; Di Micco, P.; Benada, O.; Krizan, J.; Svoboda, J.; Hulikova-Capkova, K.; Morea, V.; Boffi, A.; et al. Selective Targeting of Melanoma by PEG-Masked Protein-Based Multifunctional Nanoparticles. *Int J Nanomedicine* **2012**, *7*, 1489–1509, doi:10.2147/IJN.S28242.

43. Xu, J.; Yang, J.; Miao, Y. Dual Receptor-Targeting 99mTc-Labeled Arg-Gly-Asp-Conjugated Alpha-Melanocyte Stimulating Hormone Hybrid Peptides for Human Melanoma Imaging. *Nucl Med Biol* **2015**, *42*, 369–374, doi:10.1016/j.nucmedbio.2014.11.002.
44. Yang, J.; Guo, H.; Padilla, R.S.; Berwick, M.; Miao, Y. Replacement of the Lys Linker with an Arg Linker Resulting in Improved Melanoma Uptake and Reduced Renal Uptake of Tc-99m-Labeled Arg-Gly-Asp-Conjugated Alpha-Melanocyte Stimulating Hormone Hybrid Peptide. *Bioorg Med Chem* **2010**, *18*, 6695–6700, doi:10.1016/j.bmc.2010.07.061.
45. Zhou, Y.; Mowlazadeh Haghighi, S.; Liu, Z.; Wang, L.; Hruby, V.J.; Cai, M. Development of Ligand-Drug Conjugates Targeting Melanoma through the Overexpressed Melanocortin 1 Receptor. *ACS Pharmacol Transl Sci* **2020**, *3*, 921–930, doi:10.1021/acsptsci.0c00072.
46. Varga, J.M.; Asato, N.; Lande, S.; Lerner, A.B. Melanotropin–Daunomycin Conjugate Shows Receptor-Mediated Cytotoxicity in Cultured Murine Melanoma Cells. *Nature* **1977**, *267*, 56–58, doi:10.1038/267056a0.
47. Süli-Vargha, H.; Jeney, A.; Kopper, L.; Oláh, J.; Lapis, K.; Botyánszki, J.; Csukas, I.; Györvári, B.; Medzihradszky, K. Investigations on the Antitumor Effect and Mutagenicity of α-MSH Fragments Containing Melphalan. *Cancer Lett* **1990**, *54*, 157–162, doi:10.1016/0304-3835(90)90038-Y.
48. Chhajlani, V.; Xu, X.; Blauw, J.; Sudarshi, S. Identification of Ligand Binding Residues in Extracellular Loops of the Melanocortin 1 Receptor. *Biochem Biophys Res Commun* **1996**, *219*, 521–525, doi:10.1006/bbrc.1996.0266.
49. Garcia-Borron, J.C.; Sanchez-Laorden, B.L.; Jimenez-Cervantes, C. Melanocortin-1 Receptor Structure and Functional Regulation. *Pigment Cell Res* **2005**, *0*, 051103015727002, doi:10.1111/j.1600-0749.2005.00278.x.
50. Wallin, E.; Heijne, G. Von Genome-Wide Analysis of Integral Membrane Proteins from Eubacterial, Archaean, and Eukaryotic Organisms. *Protein Science* **1998**, *7*, 1029–1038, doi:10.1002/pro.5560070420.
51. Frändberg, P.-A.; Doufexis, M.; Kapas, S.; Chhajlani, V. Cysteine Residues Are Involved in Structure and Function of Melanocortin 1 Receptor: Substitution of a Cysteine Residue in Transmembrane Segment Two Converts an Agonist to Antagonist. *Biochem Biophys Res Commun* **2001**, *281*, 851–857, doi:10.1006/bbrc.2001.4429.
52. Sánchez-Laorden, B.L.; Sánchez-Más, J.; Turpín, M.C.; García-Borrón, J.C.; Jiménez-Cervantes, C. Variant Amino Acids in Different Domains of the Human Melanocortin 1 Receptor Impair Cell Surface Expression. *Cell Mol Biol (Noisy-le-grand)* **2006**, *52*, 39–46.
53. Medzihradszky K Synthesis and Biological Activity of Adrenocorticotropic and Melanotropic Hormones. In *Recent Developments in the Chemistry of Natural Carbon Compounds*; Bogner, R., Bruckner, R., Szantay, C., Eds.; Hungarian Academy of Science: Budapest, 1976; pp. 207–250.
54. Bregman, M.D.; Sawyer, T.K.; Hadley, M.E.; Hruby, V.J. Adenosine and Divalent Cation Effects on S-91 Melanoma Adenylate Cyclase. *Arch Biochem Biophys* **1980**, *201*, 1–7, doi:10.1016/0003-9861(80)90480-4.
55. Heward, C.B.; Yang, Y.C.S.; Ormberg, J.F.; Hadley, M.E.; Hruby, V.J. Effects of Chloramine T and Lodination on the Biological Activity of Melanotropin. *Hoppe Seylers Z Physiol Chem* **1979**, *360*, 1851–1860, doi:10.1515/bchm2.1979.360.2.1851.
56. Heward, C.B.; Yang, Y.C.S.; Sawyer, T.K.; Bregman, M.D.; Fuller, B.B.; Hruby, V.J.; Hadley, M.E. Iodination Associated Inactivation of β-Melanocyte Stimulating Hormone. *Biochem Biophys Res Commun* **1979**, *88*, 266–273, doi:10.1016/0006-291X(79)91725-X.
57. Siegrist, W.; Solca, F.; Stutz, S.; Giuffrè, L.; Carrel, S.; Girard, J.; Eberle, A.N. Characterization of Receptors for Alpha-Melanocyte-Stimulating Hormone on Human Melanoma Cells. *Cancer Res* **1989**, *49*, 6352–6358.
58. Siegfried, J.M.; Burke, T.G.; Tritton, T.R. Cellular Transport of Anthracyclines by Passive Diffusion. *Biochem Pharmacol* **1985**, *34*, 593–598, doi:10.1016/0006-2952(85)90251-5.
59. Willingham, M.C.; Cornwell, M.M.; Cardarelli, C.O.; Gottesman, M.M.; Pastan, I. Single Cell Analysis of Daunomycin Uptake and Efflux in Multidrug-Resistant and -Sensitive KB Cells: Effects of Verapamil and Other Drugs. *Cancer Res* **1986**, *46*, 5941–5946.
60. Soliman, N.; Mamdouh, D.; Elkordi, A. Choroidal Melanoma: A Mini Review. *Medicines* **2023**, *10*, 11, doi:10.3390/medicines10010011.
61. Denizot, F.; Lang, R. Rapid Colorimetric Assay for Cell Growth and Survival. *J Immunol Methods* **1986**, *89*, 271–277, doi:10.1016/0022-1759(86)90368-6.
62. Altman, F.P. Tetrazolium Salts and Formazans. *Prog Histochem Cytochem* **1976**, *9*, III–51, doi:10.1016/S0079-6336(76)80015-0.

63. Liu, Y.; Peterson, D.A.; Kimura, H.; Schubert, D. Mechanism of Cellular 3-(4,5-Dimethylthiazol-2-yl)-2,5-Diphenyltetrazolium Bromide (MTT) Reduction. *J Neurochem* **1997**, *69*, 581–593, doi:10.1046/j.1471-4159.1997.69020581.x.
64. Mosmann, T. Rapid Colorimetric Assay for Cellular Growth and Survival: Application to Proliferation and Cytotoxicity Assays. *J Immunol Methods* **1983**, *65*, 55–63, doi:10.1016/0022-1759(83)90303-4.
65. Slater, T.F.; Sawyer, B.; Sträuli, U. Studies on Succinate-Tetrazolium Reductase Systems. *Biochim Biophys Acta* **1963**, *77*, 383–393, doi:10.1016/0006-3002(63)90513-4.
66. Istivan, T.S.; Pirogova, E.; Gan, E.; Almansour, N.M.; Coloe, P.J.; Cosic, I. Biological Effects of a De Novo Designed Myxoma Virus Peptide Analogue: Evaluation of Cytotoxicity on Tumor Cells. *PLoS One* **2011**, *6*, e24809, doi:10.1371/journal.pone.0024809.
67. Kühn, J.; Shaffer, E.; Mena, J.; Breton, B.; Parent, J.; Rappaz, B.; Chambon, M.; Emery, Y.; Magistretti, P.; Depeursinge, C.; et al. Label-Free Cytotoxicity Screening Assay by Digital Holographic Microscopy. *Assay Drug Dev Technol* **2013**, *11*, 101–107, doi:10.1089/adt.2012.476.
68. Li, J.; Zhang, D.; Ward, K.M.; Prendergast, G.C.; Ayene, I.S. Hydroxyethyl Disulfide as an Efficient Metabolic Assay for Cell Viability in Vitro. *Toxicology in Vitro* **2012**, *26*, 603–612, doi:10.1016/j.tiv.2012.01.007.
69. Paulus, J.; Nachtigall, B.; Meyer, P.; Sewald, N. RGD Peptidomimetic MMAE-Conjugate Addressing Integrin AVβ3-Expressing Cells with High Targeting Index**. *Chemistry – A European Journal* **2023**, *29*, doi:10.1002/chem.202203476.
70. Overwijk, W.W.; Restifo, N.P. B16 as a Mouse Model for Human Melanoma. *Curr Protoc Immunol* **2000**, *39*, doi:10.1002/0471142735.im2001s39.
71. Teicher B.A. *Tumor Models in Cancer Research*; Teicher, B.A., Ed.; Humana Press: Totowa, NJ, 2011; ISBN 978-1-60761-967-3.